Journal of Hazardous Materials 191 (2011) 163–169

Contents lists available at ScienceDirect

Journal of Hazardous Materials

journal homepage: www.elsevier.com/locate/jhazmat

Prussian-blue-modified iron oxide magnetic nanoparticles as effective peroxidase-like catalysts to degrade methylene blue with H_2O_2

Hui Wang, Yuming Huang*

Key Laboratory of Eco-environments in Three Gorges Reservoir Region (Ministry of Education), College of Chemistry and Chemical Engineering, Southwest University, Chongqing 400715, China

ARTICLE INFO

Article history:
Received 11 January 2011
Received in revised form 13 April 2011
Accepted 14 April 2011
Available online 21 April 2011

Keywords:
Prussian-blue-modified γ-Fe_2O_3
Magnetic nanoparticles
Peroxidase-like catalyst
Methylene blue
Hydrogen peroxide

ABSTRACT

Prussian-blue (PB)-modified γ-Fe_2O_3 magnetic nanoparticles (PBMNPs) were successfully synthesized based on electric interactions between negatively charged $[Fe(CN)_6]^{4-}$ and positively charged γ-Fe_2O_3 nanoparticles. The in situ PB coating was generated by the coordinating reaction between the adsorbed $[Fe(CN)_6]^{4-}$ and the ferric ions on the surface of γ-Fe_2O_3 NPs. The as-prepared PBMNPs were characterized by FT-IR, XRD, TEM, and used to remove organic pollutants from aqueous solution, namely, using methylene blue (MB) as model compound. The experimental results showed that the target compound could be removed efficiently from solution over a wide pH range from 3 to 10 in the presence of PBMNPs as peroxidase-like catalyst and H_2O_2 as oxidant. Under optimal conditions, MB could be removed completely after 120 min of reaction at 298 K; the chemical oxygen demand (COD) removal efficiency and the total organic carbon (TOC) abatement efficiency were 53.6% and 35%, respectively. Furthermore, the PBMNPs catalysts showed high magnetization, temperature tolerance, long-term storage and operational stability, and they could be readily separated from solution by applying an external magnetic field. Finally, a possible reaction mechanism for MB degradation was also discussed.

1. Introduction

The widely used dyes in various industries such as textile, printing, rubber, food plants and cosmetics are the main source of environmental pollution and are considered as a serious threat to ecosystem. Therefore, the treatment of effluent containing dyes is of interest due to their harmful impacts on receiving waters. During the past ten years, the various conventional treatment methods, such as physical adsorption [1–3], chemical oxidation [4–6], biological degradation [7,8], have been developed for the removal of such contaminants in wastewater. However, they suffer from disadvantages including incomplete removal, high cost, disposal problem of sludge, and secondary metal ion pollution, etc. There is a growing demand for improved methods of treatment. In recent years, enzyme as biocatalyst has been widely used in wastewater treatment. For example, it has been demonstrated that horseradish peroxidase (HRP) can catalyze hydrogen peroxide to oxidize various organic compounds including phenol [9,10], chlorophenols [11], and remazol blue [12], etc. There were also attempts trying to immobilize enzymes on various matrices such as cellulose filter paper, nylon balls, and nylon tubing [13]. However, the application of natural peroxidase enzymes in the treatment of wastewater is limited due to their instability and high cost [14]. Therefore, new catalytic materials are needed for the degradation of organic pollutants such as dyes in wastewater.

Recently, Gao et al. [15] reported for the first time that Fe_3O_4 magnetite nanoparticles (FMNPs) possess intrinsic enzyme mimetic activity similar to natural peroxidases. They catalyzed the oxidation of different peroxidase substrates such as TMB (tetramethylbenzidine), DAB (di-azo-aminobenzene) and OPD (*o*-phenylenediamine) to give the same color variation as that of HRP [15]. On this basis, other studies [16,17] investigated the use of FMNPs to degrade other organic pollutants such as phenolic and aniline compounds. However, a long reaction time (6 h, at 308 K over 5 g/L FMNPs in the presence of 1.2 mol/L H_2O_2) was needed to complete the removal of two compounds due to the relatively low H_2O_2-activating ability of FMNPs [17]. In order to increase the H_2O_2-activating ability of FMNPs, ultrasonic irradiation was introduced to the preparation of FMNPs with much improved peroxidase-like catalytic ability to activate H_2O_2 [18]. In this case, only 1 h was needed for 90% removal of rhodamine B as a model compound [18]. It was reported [15] that the peroxidase-like activity of FMNPs was derived from superficial ferrous atoms of nanoparticles. Hence, there are some challenges to enhancing the peroxidase-like activity and long-term stability of FMNPs due to ease oxidation of ferrous atoms. Based on Zhang et al. [19], in this research, Prussian-blue (PB)-modified γ-Fe_2O_3 (PBMNPs) as

---

* Corresponding author. Tel.: +86 23 68254843; fax: +86 23 68254000.
E-mail addresses: yuminghuang2000@yahoo.com, ymhuang@swu.edu.cn (Y. Huang).

0304-3894/$ – see front matter © 2011 Elsevier B.V. All rights reserved.
doi:10.1016/j.jhazmat.2011.04.057

peroxidase-like catalysts were prepared, in which PB plays a role like superficial ferrous ions in FMNPs and γ-Fe_2O_3 keeps their magnetic property.

The peroxidase-like activity, high stability and convenient separation from solution by external magnetic field makes PBMNPs a potential catalyst for the degradation of organic pollutants. Here, we demonstrated that the PBMNPs could effectively degrade MB in the presence of H_2O_2. MB was selected as a model target because it is one of the most commonly used dyes and has been widely used for coloring paper, temporary hair colorant, dyeing cottons, wools, and coating for paper stock [20]. Also, it can cause burning sensation, nausea, and vomiting, mental confusion and methemoglobinemia upon ingestion [21]. Various parameters affecting the degradation, including potassium ferrocyanide, PBMNPs and H_2O_2 concentrations, pH and temperature, were investigated in detail. Furthermore, the TOC removal and the stability of PBMNPs were also studied. Finally, we proposed that the MB might be degraded by reactive oxygen species (ROS) including $^{\bullet}OH$ and $O_2^{\bullet-}$ generated during the reaction. Our results demonstrated that the PBMNPs possess excellent catalytic activity toward the oxidation of MB in the presence of H_2O_2, with advantages such as wide working pH range, easy separation, high-temperature tolerance and stability, and they may become a promising catalyst in environmental application.

2. Experimental

2.1. Chemicals and materials

Methylene blue, hydrogen peroxide, ferric chloride, sodium sulfite, ammonia, potassium ferrocyanide, potassium dichromate, silver sulfate, mercuric sulfate, sulfuric acid (98%), ammonium ferrous sulfate, 1,10-phenanthroline, ferrous sulfate, sodium hydroxide, hydrochloric acid, and *tert*-butanol were purchased from Chongqing Chemical Reagents Company (Chongqing, China). *p*-benzoquinone was obtained from Aladdin Chemistry Co. Ltd. All chemicals used in this work were of analytical grade and used as received without further purification. Ultra pure water was prepared in the lab by a water treatment device. The solution pH was adjusted using diluted HCl and NaOH solutions.

2.2. Preparation of Prussian-blue-modified γ-Fe_2O_3 magnetic nanoparticles (PBMNPs)

The method for PBMNPs preparation was adapted from Zhang et al. [19], with slight modification. Briefly, γ-Fe_2O_3 NPs were prepared by dropwisely adding 2 mL of 1 mol/L Na_2SO_3 into 3 mL of 2 mol/L $FeCl_3$ (dissolved in 2 mol/L HCl and diluted with 10.33 mL ultra pure water) within 1 min under magnetic stirring. Then a red solution appeared, indicating the formation of complex ions. When the color changed from red to light yellow, the solution was poured quickly into 80 mL of 0.85 mol/L $NH_3{\cdot}H_2O$ solution, and then vigorously stirred for 30 min. After reaction, the precipitate was washed with 0.1 mol/L HCl and separated by magnet until the pH value of the suspension was 3.0, then re-dispersed into 84 mL of water with a mass concentration of about 6 mg/mL. Then, the suspension was heated to 90 °C in 5 min and remained stirred at 100 °C for another 60 min under a stream of oxygen gas. Finally, the resulting γ-Fe_2O_3 precipitate was washed four times with ultra pure water and dried at 60 °C. For preparation of PBMNPs, the as-synthesized γ-Fe_2O_3 NPs were re-dispersed into 50 mL of water and pH was adjusted to 2.0 with 0.1 mol/L HCl. Then a proper amount of 10 mg/mL $K_4[Fe(CN)_6]{\cdot}3H_2O$ was dropwisely added to γ-Fe_2O_3 NPs under stirring. It was kept continuously stirring for 1 h, and then all the particles in the suspension were separated from the aqueous phase by magnetic separation and washed with ultra pure water three times. The resulting solids were dried at 60 °C and used for XRD, TEM, FT-IR, and catalytic degradation test. In our work, different amounts of 10 mg/mL $K_4[Fe(CN)_6]{\cdot}3H_2O$ (0.4, 0.6, 0.8, and 1 mL) were selected and added to 5 mL of γ-Fe_2O_3 NPs suspention in order to vary the PB content, and the resulting molar ratio of coated PB to core γ-Fe_2O_3 calculated by titration results (Table S1, Supporting Information) was 0.021, 0.032, 0.045 and 0.059, respectively.

2.3. Instrumentation

UV–visible measurements were performed on a UV-2450 Shimadzu spectrophotometer (Suzhou, China). The pH of the solutions was detected by a PHS-3D pH meter (Shanghai Precision Scientific Instruments Co., Ltd., China). The X-ray diffraction (XRD) patterns of the as-prepared products were measured by XD-3 X-ray diffractometer (PuXi, Beijing, China) under the conditions of nickel filtered CuKα radiation ($\lambda = 0.15406$ nm) at current of 20 mA and a voltage of 36 KV. The scanning rate was 4°/min in the angular range of 10–80° (2θ). FT-IR spectra were recorded on a Nicolet 170SX instrument (Madison, WI, USA) in the transmission mode using KBr pellets of the sample. The zeta potential measurements were performed on a Zetasizer Nano ZS90 apparatus (Malvern, UK). The size of the prepared nanoparticles was characterized by a model Hitachi H-7500 TEM operating at 80 kV accelerated voltage. Statistical analysis of TEM data revealed that the average diameter of the prepared PBMNPs was about 11 nm (Fig. 1C). Magnetic property of γ-Fe_2O_3 NPs and PBMNPs was analyzed using a vibrating sample magnetometer (VSM, HH-15). TOC measurement of supernatant after reaction was performed by a Hach IL TOC-550 Total Organic Carbon Analyzer (Hach, USA) by subtracting inorganic carbon (IC) from Total carbon (TC) which was determined using the standard curve.

2.4. Catalytic reaction experiment and analysis

The catalytic reaction experiment was carried out by adding PBMNPs into 25 mL of 20 μg/mL MB solution. After the suspension was shaken with a thermostated shaker at 180 rpm for 20 min, H_2O_2 was added to initiate the catalytic reaction. After 2 h of reaction, an Nd–Fe–B strong magnet (50 mm × 50 mm × 25 mm) was deposited at the bottom of the beaker, and the PBMNPs were isolated from the solution. The supernatant was used for MB and TOC analysis. The isolated PBMNPs were washed three times with ultra pure water and dried at 60 °C for 1 h, then used for the next cycle process.

The concentration of MB was determined by measuring the absorbance of the solution at 662 nm on a model UV-2450 spectrophotometer (Suzhou, China). The chemical oxygen demand (COD) for supernatant after reaction was measured using the conventional method [22]. The effect of free radical inhibitors was evaluated by adding *tert*-butanol (a $^{\bullet}OH$ radical scavenger) [23], and *p*-benzoquinone (a $O_2^{\bullet-}$ radicals quencher) [24,25] into reation solution.

3. Results and discussion

3.1. Characterization of PBMNPs

The PB modified MNPs were synthesized based on the electric interactions between negatively charged $[Fe(CN)_6]^{4-}$ and positively charged γ-Fe_2O_3 nanoparticles. The adsorbed $[Fe(CN)_6]^{4-}$ coordinated with the ferric ions on the surface of γ-Fe_2O_3 NPs, and resulted in the formation of a PB coating. Its further coordination with Fe^{3+} released from γ-Fe_2O_3 NPs in acidic solution (pH 2) generated more PB coating on the surface of γ-Fe_2O_3 NPs

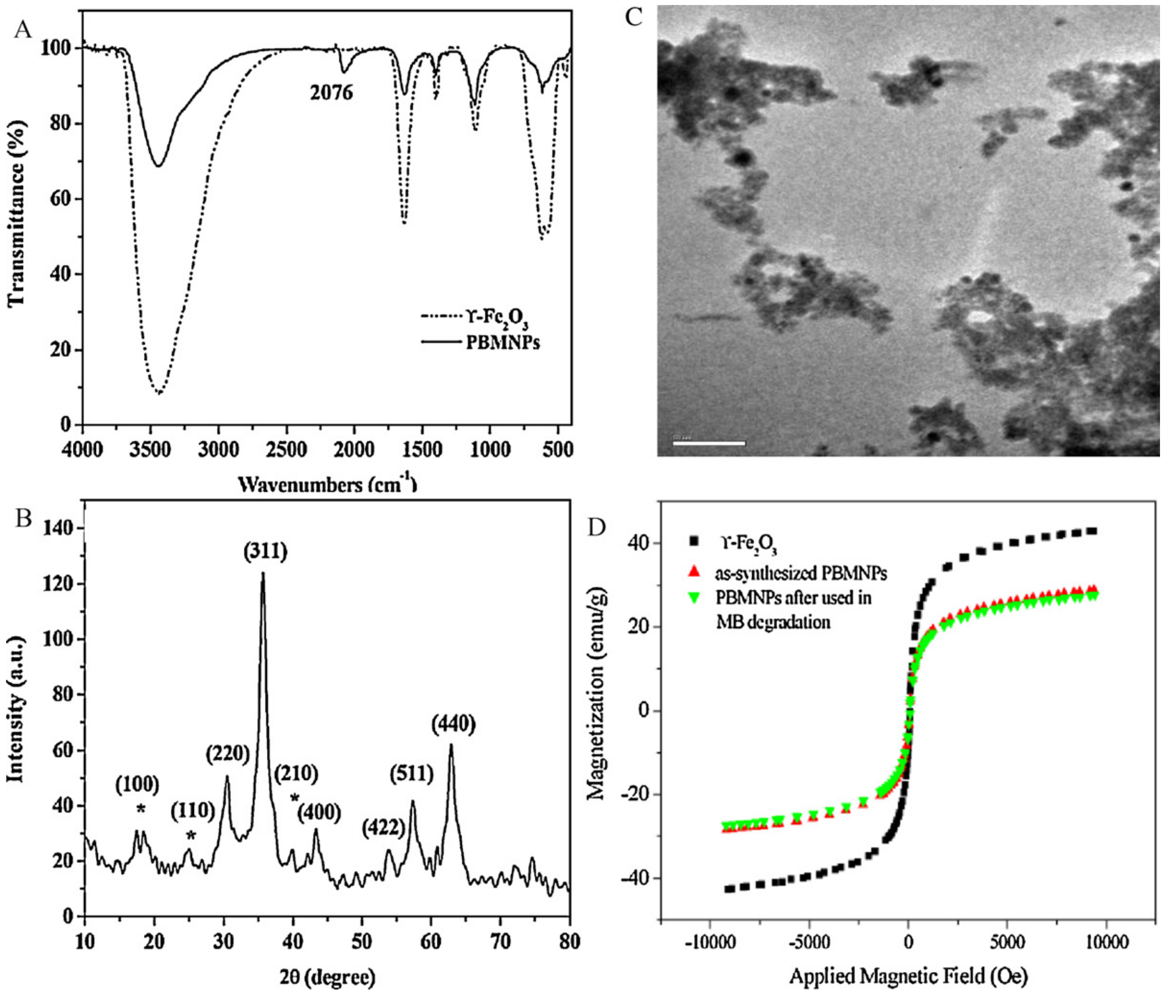

Fig. 1. (A) FT-IR spectra of γ-Fe_2O_3 NPs and PBMNPs; (B) XRD pattern of PBMNPs; (C) TEM image of PBMNPs; (D) VSM magnetization curves of γ-Fe_2O_3, the synthesized PBMNPs and PBMNPs after used in MB degradation.

[19]. In order to verify this hypothesis, we performed a series of experiments. First, we selected $FeCl_3$, which upon addition develops a blue color in aqueous solution in the presence of $K_4[Fe(CN)_6]$. As shown in Fig. S1B (Supporting Information), no significant color reaction was observed when adding $FeCl_3$ solution into the supernatant of the as-prepared PBMNPs separated by external magnetic field, suggesting that the $K_4[Fe(CN)_6]$ was completely adsorbed by γ-Fe_2O_3 NPs. Upon addition of $K_4[Fe(CN)_6]$ solution, the color change of γ-Fe_2O_3 NPs solution, from red brown to heavy blue, suggested formation of PB (Fig. S2C, Supporting Information). Second, the FT-IR was adopted to characterize the as-prepared PBMNPs as shown in Fig. 1A. The peak at 2076 cm^{-1} in the PBMNPs was assigned to the CN stretching mode [26], which indicated that PB was introduced to the surface of γ-Fe_2O_3 NPs. Third, the XRD patterns for PBMNPs were recorded and shown in Fig. 1B. The peaks of (2 2 0), (3 1 1), (4 0 0), (4 2 2), (5 1 1) and (440) were the characteristic peaks of γ-Fe_2O_3 NPs, indicating γ-Fe_2O_3 NPs are a crystalline cubic spinel structure [27]. And the peaks of (1 0 0), (1 1 0) and (2 1 0) were assigned to the characteristic peaks of PB [28], suggesting that γ-Fe_2O_3 NPs are coated with PB. The TEM image suggested a sphere-like shape of the prepared PBMNPs particles with an average diameter of about 11 nm (Fig. 1C). Fourth, the change of the zeta potentials of γ-Fe_2O_3 NPs (+23.35 mV) and PB modified γ-Fe_2O_3 NPs (PBMNPs, −0.79 mV) further demonstrated that PB is absorbed on the surface of γ-Fe_2O_3 NPs. Finally, the magnetic property of γ-Fe_2O_3 NPs before and after PB coating was evaluated. The saturation magnetization of γ-Fe_2O_3 NPs at room temperature by measuring the magnetization curve (Fig. 1D) was 47.6 emu/g; however, its decrease to 32.8 emu/g further suggested a PB coating formation on the surface of γ-Fe_2O_3 NPs. The maximal saturation magnetization of PBMNPs after use in catalytic degradation of MB was 31.9 emu/g and remained almost unchanged before and after use in catalytic degradation of MB (Fig. 1D). The experimental result shown in Fig. S2D (Supporting Information) suggested that the particles of PBMNPs are attracted quickly toward the magnet, and the reaction solution becomes limpid. This simple magnetic separation experiment proved that PBMNPs possess high magnetization. The high magnetization with large saturation magnetization makes it easy to separate PBMNPs from solution by applying an external magnetic field, which is very important for their environmental application in the removal of pollutants from a large volume of aqueous solution.

3.2. Catalytic properties of PBMNPs

Fig. 2A demonstrated the removal of MB by time in different systems. As can be seen, the removal of MB was hardly observed when H_2O_2 alone was added into MB solution, which indicated that the direct oxidation of MB by H_2O_2 was very limited. When PBMNPs were added into MB solution alone, the removal of MB was slightly increased, relative to that in the system of H_2O_2. This was probably caused by the electrostatic adsorption between the negatively charged PBMNPs (zeta potential was −0.79 mV) and the positively charged dye species. However, MB could be completely removed

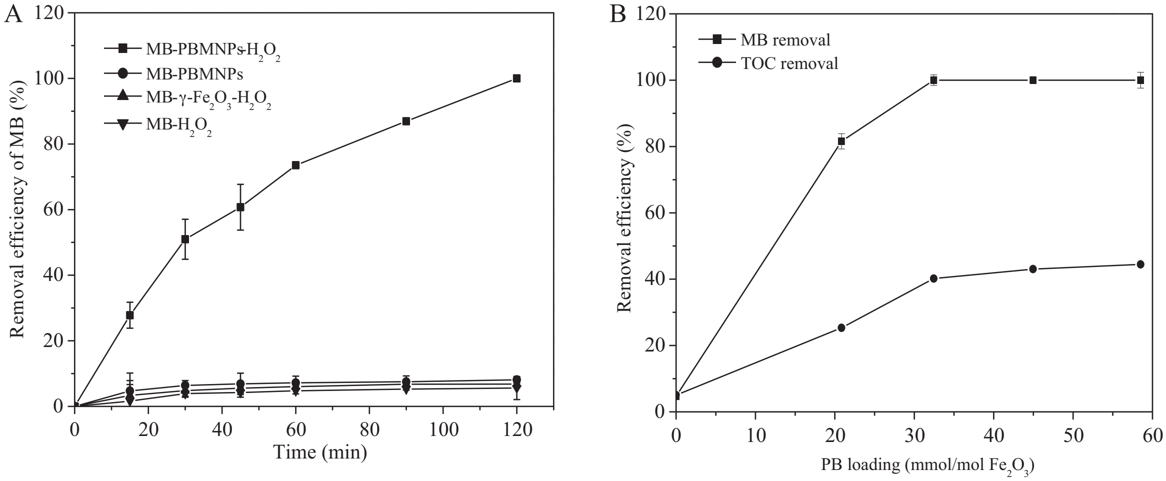

Fig. 2. (A) The catalytic properties of PBMNPs in different systems. Reaction conditions: pH 5.5, temperature 298 K, 0.3 g/L of PBMNPs or γ-Fe_2O_3, 0.4 mol/L of H_2O_2, 20 μg/mL of MB. Error bars represent one standard deviation for three measurements. (B) Effect of PB loading on MB and TOC removal. Reaction conditions: pH 5.5, temperature 298 K, 0.3 g/L of PBMNPs, 0.4 mol/L of H_2O_2, time 120 min, 20 μg/mL of MB.

after 120 min in the presence of PBMNPs and H_2O_2, showing that PBMNPs facilitated the oxidation of MB by H_2O_2. The above results imply that the degradation rather than the adsorption by PBMNPs or the oxidation by H_2O_2 plays an important role in the process of MB removal. In addition, PBMNPs exhibited much higher catalytic activity than γ-Fe_2O_3 NPs did (only about 6.81%) (Fig. 2A). The enhanced catalytic ability of the PBMNPs is attributed to the ferrous ions on their surface, which play a dominant role in the peroxidase-like activity, while the surface of γ-Fe_2O_3 NPs lacks the ferrous ions [19]. It is well known that the reactivity of a catalytic system was dependent on the catalyst load. So, we performed additional experiments to demonstrate this dependence. As shown in Fig. 2B, the catalytic activity of PBMNPs toward MB indicates PB load dependence in terms of both MB removal efficiency and TOC abatement efficiency. That is, the higher the level of PB, and the higher the catalytic activity. This phenomenon may be due to the fact that more PB provides more ferrous ions as catalytic centers to interact with substrates [19]. Complete decoloration of MB solution was reached at PB loading of 32 mmol/mol γ-Fe_2O_3. The degradation of MB in the selected conditions reached values close to 45% of TOC conversion at PB loading of 59 mmol/mol γ-Fe_2O_3, suggesting high activity of the as-prepared PBMNPs catalyst in the degradation of MB solution.

3.3. Optimization of experimental conditions

3.3.1. Effect of potassium ferrocyanide concentration

PB formation is dependent on the concentration of potassium ferrocyanide due to the fact that a PB is formed from potassium ferrocyanide and ferric ions on the surface of γ-Fe_2O_3 NPs. So, the effect of potassium ferrocyanide concentration on MB removal and TOC removal was investigated. Fig. 3 illustrates the MB adsorption and degradation with different potassium ferrocyanide concentrations. When the potassium ferrocyanide concentration increased, both the adsorption and degradation of MB on PBMNPs were enhanced. The potassium ferrocyanide concentration of 2.84 mmol/L was chosen as the optimal concentration in subsequent experiments due to the slight increase of MB degradation efficiency when the potassium ferrocyanide concentration was above 2.84 mmol/L. Also, higher concentration of potassium ferrocyanide would lead to weaker magnetism and lower concentration of potassium ferrocyanide would result in the reduction of its catalytic degradation ability, which is in agreement with the results reported elsewhere [19]. The TOC abatement efficiency showed a similar trend, but it was lower than the MB removal efficiency.

3.3.2. Effect of PBMNPs concentration

The effect of PBMNPs concentration on MB degradation and TOC removal was studied in the range from 0 g/L to 0.5 g/L. As shown in Fig. 4A, the degradation of MB increased with increasing PBMNPs concentration in the range of 0 to 0.3 g/L. A sharp increase in MB degradation was observed when the concentration of PBMNPs was lower than 0.3 g/L. However, only slight changes in MB degradation were observed when the concentration of PBMNPs was above 0.3 g/L. TOC abatement efficiency increased slowly with PBMNPs concentration above 0.2 g/L. When the concentration of PBMNPs reached to 0.3 g/L, MB could be removed completely, but only about 30% TOC was abated. Furthermore, the PBMNPs could be quickly separated within 1 min by a magnet after the degradation test was finished, which makes PBMNPs suitable for economical operation in industrial wastewater treatment.

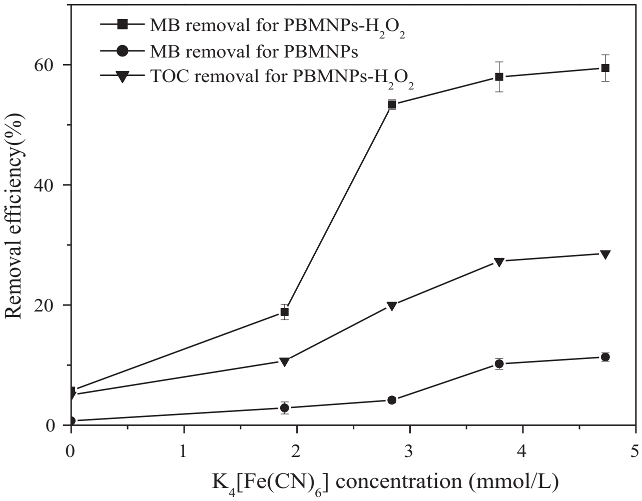

Fig. 3. Effect of potassium ferrocyanide concentration on MB removal and TOC removal. Reaction conditions: pH 5.5, time 60 min, temperature 298 K, 0.3 g/L of PBMNPs, 0.4 mol/L of H_2O_2, 20 μg/mL of MB. Error bars represent one standard deviation for three measurements.

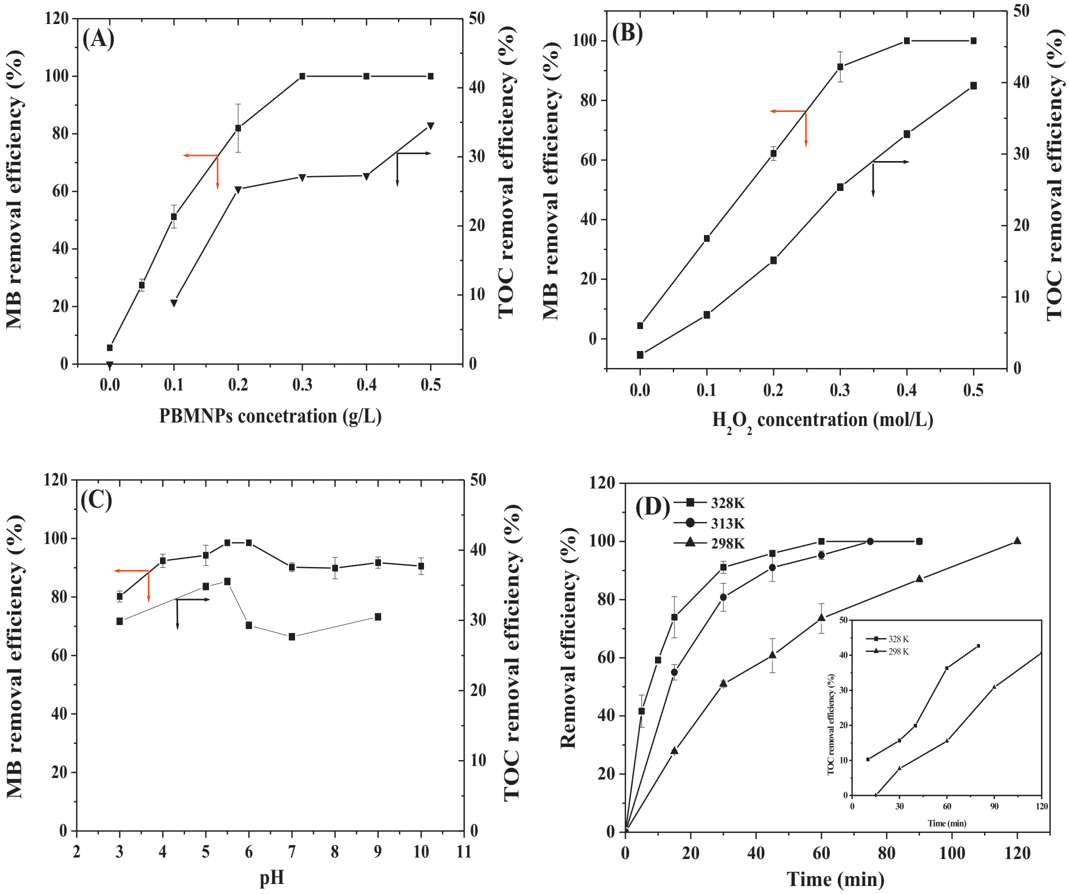

Fig. 4. Effects of reaction conditions on MB removal and TOC removal. (A) Effect of PBMNPs concentration. Reaction conditions: pH 5.5, time 120 min, temperature 298 K, 0.4 mol/L of H_2O_2, 20 μg/mL of MB. (B) Effect of H_2O_2 concentration. Reaction conditions: pH 5.5, time 120 min, temperature 298 K, 0.3 g/L of PBMNPs, 20 μg/mL of MB. (C) Effect of pH. Reaction conditions: time 120 min, temperature 298 K, 0.4 mol/L of H_2O_2, 0.3 g/L of PBMNPs, 20 μg/mL of MB. (D) Effect of temperature. Reaction conditions: pH 5.5, time 120 min, 0.4 mol/L of H_2O_2, 0.3 g/L of PBMNPs, 20 μg/mL of MB. Error bars represent one standard deviation for three measurements.

3.3.3. *Effect of H_2O_2 concentration*

It has been demonstrated that MNPs require a higher H_2O_2 concentration to reach the maximal level of peroxidase activity, compared with natural enzyme such as HRP [15]. A similar trend was also observed in our study. The dependence of degradation efficiency of MB and TOC removal on H_2O_2 concentration was investigated and is shown in Fig. 4B. It was expected that the adsorption of MB by PBMNPs was low in the absence of H_2O_2. The experimental results showed that the degradation efficiency of MB increased rapidly with increasing concentration of H_2O_2 in the range of 0–0.3 mol/L. However, only slight changes in MB removal were observed when the concentration of H_2O_2 was above 0.3 mol/L. TOC removal increased rapidly with increasing concentration of H_2O_2 in the range of 0–0.5 mol/L. Considering that the removal of MB was 100% when the concentration of H_2O_2 reached to 0.4 mol/L, the level of 0.4 mol/L of H_2O_2 was selected in subsequent experiments.

3.3.4. *Effect of pH*

The effect of pH on the degradation efficiency of MB was examined in the range of 3–10. As can be seen from Fig. 4C, the MB degradation worked very effectively over a wide pH range from 3 to 10, which is very favorable to the practical treatment of wastewater because there is no need to adjust the solution pH. The maximum MB degradation occurred at pH 5.5 to pH 6, which is consistent with the results reported elsewhere [29]; however, it is unlike the typical Fenton reaction and modified Fenton reaction for phenol degradation, which was usually performed at pH 3.0 [17]. This means that Prussian-blue-modified iron oxide magnetic nanoparticles could improve the pH tolerance of magnetic nanoparticles. At pH below 5.5 or pH above 6, the degradation efficiency of MB decreased. The TOC abatement efficiency increased with the increase of pH from 3.0 to 5.5 and reached about 35% at pH 5.5. When pH ranged from above 5.5–10, the TOC abatement decreased slightly to about 30%. This may be due to the competitive adsorption between proton and MB or to the scavenging effect of the $^{\bullet}OH$ radical by H^+ at lower pH and the instability of H_2O_2 at higher pH [17,30].

3.3.5. *Effect of temperature*

Temperature plays an important role in most chemical reactions. This work studied the effect of temperature between 298 K and 328 K on the degradation efficiency of MB. The temperature was controlled by the thermostatic water bath. The degradation efficiency of MB and TOC removal by time at different temperatures were plotted. The results in Fig. 4D demonstrated that the degradation efficiency of MB and TOC removal are higher at higher temperatures within the tested temperature range. The reaction time needed for complete removal of MB dropped from 120 min to 60 min with the temperature increasing from 298 K to 328 K. And the TOC abatement efficiency increased from about 30% to about 45% after 80 min reaction. Also, the experimental results suggested that the catalytic activity of the as-prepared PBMNPs keeps unchanged even at a high-temperature (328 K), showing the high-temperature tolerance of PBMNPs, which is impossible for most natural enzymes due to denaturation at higher temperatures [31]. For operational convenience, 298–303 K (room temperature) was

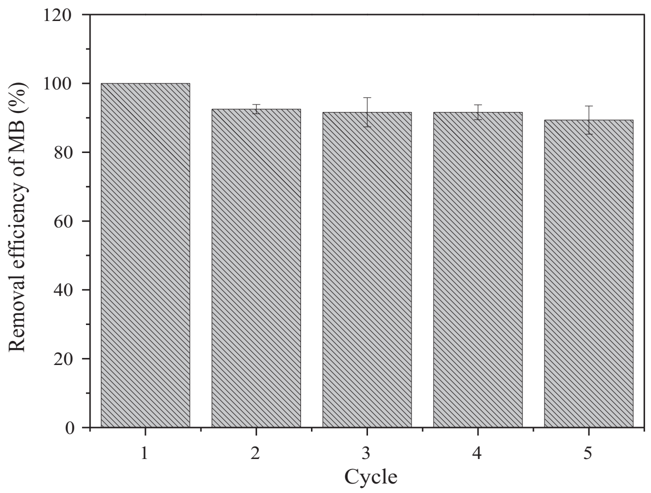

Fig. 5. Catalytic activity of PBMNPs over various cycles of re-utilization using identical reaction conditions. Reaction conditions: pH 5.5, time 120 min, temperature 298 K, 0.3 g/L of PBMNPs, 0.4 mol/L of H_2O_2, 20 μg/mL of MB. Error bars represent one standard deviation for three measurements.

chosen as the experimental temperature range for all subsequent experiments.

In summary, the optimized conditions for MB removal using the PBMNPs–H_2O_2 system were as follows: 0.4 mol/L H_2O_2, 0.3 g/L PBMNPs, pHs from 5.5 to 6.0, temperatures from 298 K to 303 K, reaction time of 120 min. The MB could be removed completely, and the chemical oxygen demand (COD) removal efficiency and the TOC abatement efficiency were 53.6% (Fig. S3, Supporting information) and about 35% under the above conditions, respectively.

3.4. Stability of PBMNPs

The operational stability of the as-prepared PBMNPs was explored by checking the cycle number dependence of MB degradation for 20 μg/mL MB, using the same PBMNPs separated by the magnet for subsequent cycles. The results in Fig. 5 demonstrated that about 90% MB removal was held after a five-cycle run of the PBMNPs. This shows that PBMNPs are stable and can be used for repeated treatment of dyes such as MB. The decrease in MB degradation may be due to the loss and aggregation of PBMNPs during the cycling process, and the adsorption of MB or intermediates on the surface of PBMNPs. To further ascertain the storage stability of the as-prepared PBMNPs, the MB degradation experiment was performed with the PBMNPs stored for 110 days since their first preparation. 100% removal of MB was also obtained, demonstrating very good stability and activity of the PBMNPs.

3.5. A possible reaction mechanism

It has been reported that $^{\bullet}OH$ and $O_2^{\bullet -}$ radicals are important intermediates in the H_2O_2–Fe_3O_4 system for the degradation of organic pollutants [16,18,29]. In order to investigate the possible active intermediates in the present reaction system, *p*-benzoquinone (BQ) and *tert*-butyl alcohol (TBA) were selected, because it has been reported that BQ is a good trapper for $O_2^{\bullet -}$[24,25], and TBA can react with $^{\bullet}OH$ [23]. The results suggested that MB degradation is inhibited in the presence of BQ or TBA; however, it is only partially suppressed in the presence of TBA (Fig. S4, Supporting information). For example, the degradation of MB decreased to only about 22% when 0.13 mol/L TBA was added; however, the degradation of MB dropped to about 45.6% when only 1 mmol/L BQ was added. The results demonstrated that although $O_2^{\bullet -}$ and $^{\bullet}OH$ radicals are formed in the catalytic degradation of MB by H_2O_2 in the presence of PBMNPs, the $O_2^{\bullet -}$ radical is probably the mainly reactive intermediate. The produced $O_2^{\bullet -}$ and $^{\bullet}OH$ radicals react with MB to initiate the degradation and subsequently mineralization of MB. The $O_2^{\bullet -}$ radical and $^{\bullet}OH$ radical were probably formed by H_2O_2, which was firstly adsorbed onto the surface of PBMNPs, and then activated by the bound ferrous iron (from PBMNPs) and Fe^{3+} [18]. It is also possible that PBMNPs as the catalysts could catalyze the decomposition of H_2O_2 to yield active intermediates such as $^{\bullet}OH$ and $O_2^{\bullet -}$ [32–34].

4. Conclusion

In summary, a PBMNPs-based degradation method has been developed for the removal of MB as a model target with PBMNPs as a catalyst and H_2O_2 as an oxidant in the present study. The in situ PB coating formation on the surface of γ-Fe_2O_3 NPs with addition of negatively charged $[Fe(CN)_6]^{4-}$ was characterized by the presence of blue color development on the surface of γ-Fe_2O_3 NPs, FT-IR, XRD, and the change of the zeta potential of γ-Fe_2O_3 NPs. The Prussian-blue-modified γ-Fe_2O_3 NPs showed excellent catalytic activity toward the oxidation of MB in the presence of H_2O_2, producing a highly efficient removal for MB, which is attributed to the formation of highly reactive oxygen species such as $^{\bullet}OH$ and $O_2^{\bullet -}$ radicals. This result demonstrated a relatively high H_2O_2-activating ability of PBMNPs. The MB could be removed completely after a 120 min reaction with the COD removal efficiency of 53.6% and TOC removal efficiency of 35% under optimal conditions. Our conclusion is that the PBMNPs may become a promising catalyst in environmental applications owing to their wide working pH range (pH 3–10), temperature tolerance, long-term storage and operational stability.

Acknowledgements

The financial support of the research by the Natural Science Foundation (no. 21075099) and the 211 Project of Southwest University (the Third Term) are gratefully acknowledged.

Appendix A. Supplementary data

Supplementary data associated with this article can be found, in the online version, at doi:10.1016/j.jhazmat.2011.04.057.

References

[1] S.S. Azhar, A.G. Liew, D. Suhardy, K.F. Hafiz, M.D.I. Hatim, Dye removal from aqueous solution by using adsorption on treated sugarcane bagasse, Am. J. Appl. Sci. 2 (2005) 1499–1503.

[2] V.J. Vilar, C.M. Botelho, R.A. Boaventura, Methylene blue adsorption by algal biomass based materials: biosorbents characterization and process behaviour, J. Hazard. Mater. 147 (2007) 120–132.

[3] M. Hirata, N. Kawasaki, T. Nakamura, K. Matsumoto, M. Kabayama, T. Tamura, S. Tanada, Adsorption of dyes onto carbonaceous materials produced from coffee grounds by microwave treatment, J. Colloid Interface Sci. 254 (2002) 17–22.

[4] A. Ventura, G. Jacquet, A. Bermond, V. Camel, Electrochemical generation of the Fenton's reagent: application to atrazine degradation, Water Res. 36 (2002) 3517–3522.

[5] L.W. Lackey, R.O. Mines, P.T. McCreanor, Ozonation of acid yellow 17 dye in a semi-batch bubble column, J. Hazard. Mater. 138 (2006) 357–362.

[6] M.F. Sevimll, C. Kinaci, Decolorization of textile wastewater by ozonation and Fenton's process, Water Sci. Technol. 45 (2002) 279–286.

[7] O.D. Olukanni, A.A. Osuntoki, D.C. Kalyani, G.O. Gbenle, S.P. Govindwar, Decolorization and biodegradation of Reactive Blue 13 by Proteus mirabilis LAG, J. Hazard. Mater. 184 (2010) 290–298.

[8] S. Venkata Mohan, N. Chandrasekhar Rao, K. Krishna Prasad, J. Karthikeyan, Treatment of simulated Reactive Yellow 22 (Azo) dye effluents using Spirogyra species, Waste Manage. 22 (2002) 575–582.

[9] V.A. Cooper, J.A. Nicell, Removal of phenols from a foundry wastewater using horseradish peroxidase, Water Res. 30 (1996) 954–964.

[10] J. Dec, J.M. Bollag, Use of plant-material for the decontamination of water pollution of water polluted with phenols, Biotechnol. Bioeng. 44 (1994) 1132–1139.

[11] K. Tatsumi, S. Wada, H. Ichikawa, Removal of chlorophenols from wastewater by immobilized horseradish peroxidase, Biotechnol. Bioeng. 51 (1996) 126–130.

[12] A. Bhunia, S. Durani, P.P. Wangikar, Horseradish peroxidase catalyzed degradation of industrially important dyes, Biotechnol. Bioeng. 72 (2001) 562–567.

[13] M.H. Siddique, C.C. St Pierre, N. Biswas, J.K. Bewtra, K.E. Taylor, Immobilized enzyme catalyzed removal of 4-chlorophenol from aqueous solution, Water Res. 27 (1993) 883–890.

[14] M. Hamid, Khalil-ur-Rehman, Potential applications of peroxidases, Food Chem. 115 (2009) 1177–1186.

[15] L.Z. Gao, J. Zhuang, L. Nie, J.B. Zhang, Y. Zhang, N. Gu, T.H. Wang, J. Feng, D.L. Yang, S. Perrett, X. Yan, Intrinsic peroxidase-like activity of ferromagnetic nanoparticles, Nat. Nanotechnol. 2 (2007) 577–583.

[16] S.X. Zhang, X.L. Zhao, H.Y. Niu, Y.L. Shi, Y.Q. Cai, G.B. Jiang, Superparamagnetic Fe_3O_4 nanoparticles as catalysts for the catalytic oxidation of phenolic and aniline compounds, J. Hazard. Mater. 167 (2009) 560–566.

[17] J.B. Zhang, J. Zhuang, L.Z. Gao, Y. Zhang, N. Gu, J. Feng, D.L. Yang, J.D. Zhu, X.Y. Yan, Decomposing phenol by the hidden talent of ferromagnetic nanoparticles, Chemosphere 73 (2008) 1524–1528.

[18] N. Wang, L. Zhu, D. Wang, M. Wang, Z. Lin, H. Tang, Sono-assisted preparation of highly-efficient peroxidase-like Fe_3O_4 magnetic nanoparticles for catalytic removal of organic pollutants with H_2O_2, Ultrason. Sonochem. 17 (2010) 526–533.

[19] X.Q. Zhang, S.W. Gong, Y. Zhang, T. Yang, C.Y. Wang, N. Gu, Prussian blue modified iron oxide magnetic nanoparticles and their high peroxidase-like activity, J. Mater. Chem. 20 (2010) 5110–5116.

[20] V. Vadivelan, K.V. Kumar, Equilibrium, kinetics, mechanism, and process design for the sorption of methylene blue onto rice husk, J. Colloid Interface Sci. 286 (2005) 90–100.

[21] M. Rafatullah, O. Sulaiman, R. Hashim, A. Ahmad, Adsorption of methylene blue on low-cost adsorbents: a review, J. Hazard. Mater. 177 (2010) 70–80.

[22] State Environmental Protection Administration, The editoral board of Water and wastewater monitoring and analysis methods, water and wastewater monitoring and analysis methods, fourth ed., Beijing, China, 2002, pp. 210–213.

[23] K. Ishibashi, A. Fujishima, T. Watanabe, K. Hashimoto, Quantum yields of active oxidative species formed on TiO_2 photocatalyst, J. Photochem. Photobiol., A: Chem. 134 (2000) 139–142.

[24] L.E. Manring, M.K. Kramer, C.S. Foote, Interception of O_2^- by benzoquinone in cyanoaromatic-sensitized photooxygenations, Tetrahedron Lett. 25 (1984) 2523–2526.

[25] E. Hayon, M. Simic, Acid-base properties of free radicals in solution, Acc. Chem. Res. 7 (1974) 114–121.

[26] J.B. Ayers, W.H. Waggoner, Synthesis and properties of two series of heavy metal hexacyanoferrates, J. Inorg. Nucl. Chem. 33 (1971) 721–733.

[27] Y.K. Sun, M. Ma, Y. Zhang, N. Gu, Synthesis of nanometer-size maghemite particles from magnetite, Colloids Surf., A 245 (2004) 15–19.

[28] S.Q. Liu, J.J. Xu, H.Y. Chen, Electrochemical behavior of nanosized Prussian blue self-assembled on Au electrode surface, Electrochem. Commun. 4 (2002) 421–425.

[29] N. Wang, L.H. Zhu, M.Q. Wang, D.L. Wang, H.Q. Tang, Sono-enhanced degradation of dye pollutants with the use of H_2O_2 activated by Fe_3O_4 magnetic nanoparticles as peroxidase mimetic, Ultrason. Sonochem. 17 (2010) 78–83.

[30] C.L. Hsueh, Y.H. Huang, C.C. Wang, C.Y. Chen, Degradation of azo dyes using low iron concentration of Fenton and Fenton-like system, Chemosphere 58 (2005) 1409–1414.

[31] J.Z. Liu, T.L. Wang, L.N. Ji, Enhanced dye decolorization efficiency by citraconic anhydride-modified horseradish peroxidase, J. Mol. Catal. B: Enzym. 41 (2006) 81–86.

[32] S.F. Li, X.M. Zhang, W.X. Du, Y.H. Ni, X.W. Wei, Chemiluminescence reactions of a luminol system catalyzed by ZnO nanoparticles, J. Phys. Chem. C 113 (2009) 1046–1051.

[33] S.L. Xu, H. Cui, Luminol chemiluminescence catalysed by colloidal platinum nanoparticles, Luminescence 22 (2007) 77–87.

[34] S.H. He, W.B. Shi, X.D. Zhang, J. Li, Y.M. Huang, β-cyclodextrins-based inclusion complexes of $CoFe_2O_4$ magnetic nanoparticles as catalyst for the luminol chemiluminescence system and their applications in hydrogen peroxide detection, Talanta 82 (2010) 377–383.